ACADEMIC PRESS

Available online at www.sciencedirect.com

SCIENCE DIRECT®

Journal of Magnetic Resonance 163 (2003) 16–22

JMR Journal of Magnetic Resonance

www.elsevier.com/locate/jmr

A PGSE study of propane gas flow through model porous bead packs

S.L. Codd* and S.A. Altobelli

New Mexico Resonance, Albuquerque, NM, USA

Received 13 November 2002; revised 24 February 2003

Abstract

We present a study of the probability density for molecular displacements of gas flowing through bead packs. The three bead packs to be described are composed of polydispersed porous PVC particles, 500 μm glass spheres, and 300 μm polystyrene spheres. A range of velocities (1 cm s^{-1} to 1 m s^{-1}) and observation times (3–500 ms), hence transport distances, are presented. For comparison we also measure the propagators for water flow in the polystyrene sphere pack.

The exchange time between the moving and the stagnant portions of the flow is a strong function of the diffusion coefficient of the fluid. Comparing the propagators between water and propane flowing in similar porous media makes this clear. The gas propagators, for flowing and diffusing molecules, consistently show a feature at the average pore diameter. This feature has previously been observed for similar Peclet number studies in smaller monodispersed bead packs using liquids, but is now demonstrated for larger beads with gas. We analyze and discuss these propagators in the physically intuitive propagator space and also in the well-understood Fourier q space.

The extension of NMR PGSE experiments to gas systems allows flow and diffusion information to be obtained over a wider range of length and time scales than with liquids, and also for a new range of physical environments and systems. Interactions between stochastic and deterministic motion are fundamental to the theoretical description of transport in porous media, and the time and length scale dependences are central to an understanding of the resultant dispersive motion.

Keywords: Gas phase NMR; PGSE NMR; Propagators; Diffusive diffraction; Holdup dispersion

1. Introduction

Flow in porous media is highly relevant to the oil and gas industries, understanding of mass transfer in geological media, and process control in chromatography columns and catalytic burners. NMR Microscopy techniques and, in particular, pulsed gradient spin echo (PGSE) experiments, are uniquely suited for spatially resolved studies of concentration, flow, and diffusion in liquid phase flow through porous media [1]. In addition, the opacity of such systems render optical techniques difficult to apply. Recently, a few groups have sought to extend the range of situations in which NMR microscopy techniques can be applied through the use of various gases [2–6]. The results have yielded complementary information to that obtained from other porosimetry methods, including liquid state NMR.

The immediate problem facing experimentalists wishing to study gas flow with NMR, is the reduced density of the gases and hence the reduced signal. Laser-polarized noble gases can now be used, with enhanced nuclear spin polarization of >10%, to compensate for this loss. Although limitations still exist, the most restrictive being the added complexity of gas polarization, cost, and the strong effects of surface relaxation on T_1, useful high-resolution images and velocity maps have been obtained [3,4].

At New Mexico Resonance we are exploring the advantages of using thermally polarized fluorinated gases, such as C_2F_6 and protonated gases, such as C_2H_6. Multiple NMR active nuclei per molecule can provide significant signal enhancement, short T_1s for the spherical fluorinated molecules allow increased signal aver-

* Corresponding author. Present address: Department of Chemical Engineering, Montana State University, 306 Cobleigh Hall, P.O. Box 173920, Bozeman, MT 59717, USA. Fax: 1-1406-994-5308.

E-mail address: Scodd@coe.montana.edu (S.L. Codd).

1090-7807/03/$ - see front matter © 2003 Elsevier Science (USA). All rights reserved.
doi:10.1016/S1090-7807(03)00111-3

aging, and pressurizing the system not only increases signal but also allows pressure dependent studies. The advantages of this approach over hyperpolarized gases are primarily the ease of preparation and well-defined magnetization. Furthermore the possibility to analyze multiple gases and their interactions with each other and solid surfaces has yielded some interesting applications [7–9]. Thermal polarization allows the use of standard NMR sequences, long duration experiments and simple continuous gas flow systems. Finally, hydrocarbon gases are cheap and readily available, although they are flammable. The hydrocarbon gas approach was pioneered at the International Tomography Center, Novosibirsk, Russia, where they are investigating gas flow through catalysts [5,8].

Flow in porous media is ideally suited to pulsed gradient NMR techniques. The ability to obtain fully resolved propagators as a function of observation times [10], in multiple directions [11] and in addition to relaxation time [12] has allowed detailed studies of a variety of model and industrially significant liquid systems [8,13,14]. Far fewer PGSE NMR studies have looked at gas transport in porous media. It has been demonstrated that hydrocarbon gas flow through glass beads and silica beads can indeed be investigated using the PGSE propagator experiment [5]. In this work, we present propagators that clearly show the evolution of the flowing and stagnant regions of the flow, as have previously been presented for liquid flows [15]. In the porous PVC particles, the evolution of the stagnant peak due to gas trapped in dead-end pores is almost independent of the bulk flow rate. On the other hand, in the spherical bead packs the exchange of gas into the flow paths is faster and strongly influenced by diffusion and the flow rate. We present analysis of these data in both the propagator space and the Fourier q space [1,10].

2. Transport measurements using PGSTE NMR

Fig. 1 shows the pulsed gradient stimulated echo sequence (PGSTE) used to acquire the data in this work.

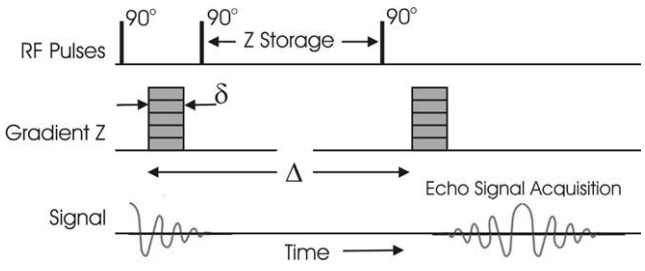

Fig. 1. The pulsed gradient stimulated echo sequence. Varying the gradient strength samples q space. The observation time is determined by setting the gradient pulse separation time Δ.

The sequence includes two gradient pulses of strength $\mathbf{g}$ and duration δ separated by the observation time Δ. This sequence is a member of an extensive family of displacement encoding and velocity exchange encoding pulsed field gradient experiments, and a detailed description of the full capabilities of these types of experiments can be found elsewhere [1,10,11,16]. In the simple PGSTE experiment, if the narrow pulse assumption is valid, i.e., the gradient duration δ is less than the characteristic time of the motion across the pore, then there exists a Fourier relationship between the conditional propagator $P_S(Z,\Delta)$ and the echo attenuation $E(q)$, where $q = \gamma\delta\mathbf{g}/2\pi$.

$$E(q,\Delta) = \int\int \rho(z,0)P_S(z|z',\Delta)\exp(\mathrm{i}2\pi q(z-z'))\,\mathrm{d}z\,\mathrm{d}z'. \tag{1}$$

In other words, the experiment encodes the signal for the displacement Z, which occurs during the pulse separation Δ. If large enough gradients are available, then it is possible to obtain fully resolved displacement propagators, giving a detailed and easily interpretable visualization of the underlying physics of motion in the system. If gradient strength is insufficient for the significant distance scale, then useful information on effective diffusion or mean flow can still be obtained from the small gradient values, i.e., the low q space data.

3. Gas transport in porous media

Transport in porous media is complex due to the detailed streamline pattern. An understanding of the various dispersion mechanisms combined with a numerical simulation is necessary to predict the behavior in both model bead packs and natural materials. Experimental data can validate these predictions or indicate deficiencies. Dispersion is a combination of several basic transport mechanisms, which will be briefly outlined here; a fuller description can be found elsewhere [17]. In fluid flow through a bead pack there are three dispersion mechanisms: Taylor dispersion, mechanical dispersion, and 'hold-up' dispersion. Taylor dispersion is enhanced dispersion due to molecular self-diffusion across adjacent advection paths and is driven by stochastic Brownian motion. It scales as Pe^2 [18] where Pe is the Peclet number, a measure of the ratio of convective to diffusive forces. The Peclet number is defined as $Pe = v_{av}d/D_0$, where d is the bead diameter, v_{av} is the average velocity in the pores, and D_0 is the fluid self-diffusion coefficient. In porous media the advection paths are tortuous and involve multiple bifurcations, resulting in stochastic variations in the velocities of particles. This process is often called 'mechanical dispersion' which scales as Pe. The third dispersion mech-

anism, 'hold-up dispersion' results from particles that are trapped in stagnant regions of the flow such as dead-end pores or separated regions which reenter the backbone flow through self-diffusion (or very slow flows). The scaling of this mechanism is $Pe\log(Pe)$. For Peclet numbers higher than 1 this process is much slower than advection and a stagnant peak can be seen in the propagator.

The data in this paper are displayed using the propagator formalism, where the propagator $P_\Delta(\mathbf{R})$ is the probability distribution of displacements $\mathbf{R} = \mathbf{r}(\Delta) - \mathbf{r}(0)$ in time Δ. The effective dispersion at time Δ is indicated by the width of the propagator, whereas the offset of the propagator indicates the average displacement over time Δ. This discussion is appropriate for both liquid and gas flows. However, for the same porous medium and flow rate, the higher diffusivity of gas leads to a Peclet regime that is about 1000 times smaller than for liquid. The Reynolds number Re is a measure of the ratio of inertial to viscous forces $Re = v_{av}d/\nu$, where ν is the kinematic viscosity. For a fixed Peclet number the Reynolds number will typically be several orders of magnitude higher in the gas flow compared to the liquid flow. Therefore, inertial forces must be taken into account in modeling such flows.

4. Experiment

A number of different systems and configurations are compared in this study. The flow and dispersion of propane gas was observed in three different bead packs: 300 μm (±100 μm) polystyrene spheres, 500 μm (±100 μm) glass spheres, and polydisperse porous conglomerated PVC particles with average diameter of 100 μm. For comparison, water transport through the polystyrene bead pack was also studied. A 4 cm internal diameter column ensured a column to bead diameter ratio of over 80. The RF coil was placed at a sufficient distance from the entrance points to ensure an even distribution of the streamlines, and images showed no indication of the presence of jet stream flow. The water flow was driven by a gravity feed system with a constant pressure head of 3 m. The gas flow was driven by a peristaltic Masterflex pump in a continuous flow set-up. For the highest gas flow rate, with a velocity of $1\,\mathrm{m\,s^{-1}}$, the gas was driven directly from the cylinder, but for all the other flows the pump could provide sufficient pressure. To increase the available signal, the gas was input at a pressure of 170 kPa in the sample. The pressure was monitored and did not vary over the duration of an experiment.

The NMR experiments were performed on an TecMag Libra spectrometer (Tecmag, Houston, TX) attached to a 1.9 T 31 cm Oxford magnet, with a gradient coil made by Resonance Research that produces maximum gradient strengths of $30\,\mathrm{G\,cm^{-1}}$. In order to reduce strong background gradient effects, the stimulated-echo version of the pulsed field gradient sequence (PGSTE) was used, as shown in Fig. 1. Gradient strengths were varied with a constant gradient duration (δ) of 950 μs for the gas flows, and 2 ms for the water flow. For the fastest moving spins these gradient durations may not be in the narrow pulse approximation regime, but the slower spins, i.e., those parts of the propagators at the smaller displacements, can be understood with narrow pulse approximations. All displacements shown in this paper correspond to movements parallel to the direction of flow, along the axis of the magnet.

5. Results and discussion

Many NMR propagator data have been obtained in the last 10 years from liquid diffusing and flowing in model bead packs of monodispersed polymer or glass spheres [19–23]. These studies have become progressively more complicated involving multi-dimensional spatial and temporal components [16], studies of two-phase (oil and water) mixtures [14] as well as extending the media to include porous chromatography column spheres [15].

To give an idea of how the structure of our polystyrene bead pack may compare to other bead packs, we show in Fig. 2. propagators for diffusing water in the 300 μm beads (Fig. 2a) and for water flowing at a rate corresponding to $v_{av} = 13\,\mathrm{mm\,s^{-1}}$, $Pe = 1700$, $Re = 0.5$ (Fig. 2b).

When the water diffuses, even at 1.2 s the molecules are not significantly affected by the 300 μm diameter pore boundaries. However, as has been observed before, when the water is flowing and has been transported over distances greater than the pore dimensions, the pore structure influences the propagator at displacements corresponding to the pore size. Perhaps this is due to the fact that the sizes of the stagnant regions in the flow are related to the average pore size. In other words, we may consider that once a molecule has diffused into the main streamline flow it will quickly be dispersed and be included in the broad flowing Gaussian portion of the propagator. The transition between the stagnant regions of the flow and the faster flowing streamlines can be observed in the time series of data shown in Fig. 2b.

In the PGSTE experiment, we sample the moving spins with successively larger gradient pulses of a fixed duration δ and a fixed separation Δ. The parameter $q = \gamma\delta\mathbf{g}/2\pi$ is directly related to these experiment parameters. If we can sample out to high values in q space, i.e., if large enough gradients are available, then the data can be displayed in propagator space. This is analogous to analyzing image data in the spatial domain rather than trying to interpret the image shape from the

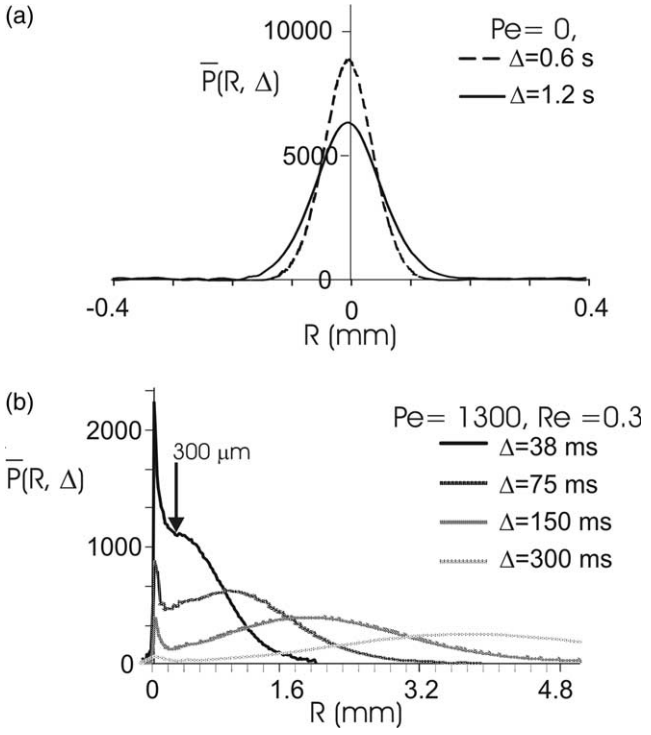

Fig. 2. (a) Water diffusing in 300 μm polystyrene beads. Even at an observation time $\Delta = 1.2$ s the molecules have still not experienced the pore walls due to the small diffusion coefficient of $2.3 \times 10^{-9}\,m^2\,s^{-1}$. (b) Water flowing at $1.3\,cm\,s^{-1}$ in 300 μm polystyrene beads. At this faster flow, we can see the hold-up due to molecules trapped in stagnant regions. The stagnant peak disappears over a time corresponding to the maximum distance a molecule may have to diffuse in order to reach the main flow, i.e., a pore diameter.

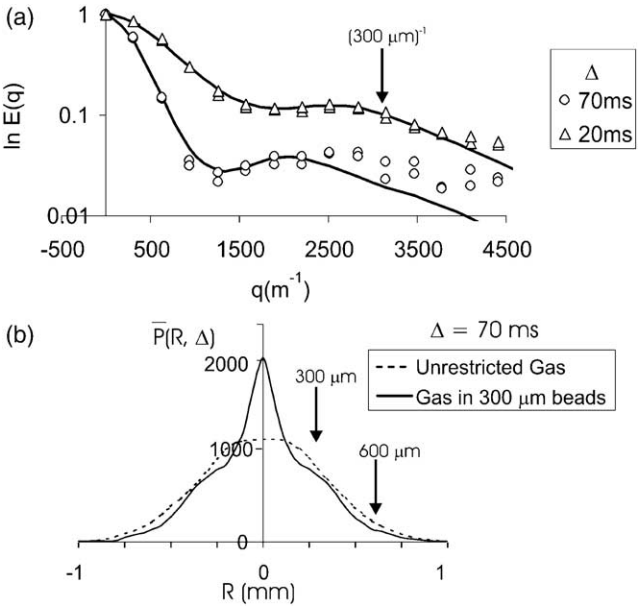

Fig. 3. (a) Diffraction patterns from gas diffusing in 300 μm polystyrene beads at two observation times, $\Delta = 20$ and 70 ms. These q space diffraction peaks have previously been observed for water diffusing in smaller (10–100 μm) beads [24]. The solid lines are fits obtained using the pore-hopping theory described in this paper and the fit parameters are listed in Table 1. (b) The data in Fig. 3a are Fourier transformed to give the propagator representation. The propagator for the gas diffusing in 300 μm polystyrene beads is compared with the Gaussian propagator obtained for unrestricted gas. The interaction with the pore walls can be seen.

original k space experiment domain. The q space data, or echo attenuation $E(q,\Delta)$ data, are related via a Fourier transform to the propagator $P_\Delta(\mathbf{R})$ that was previously described [1]. However, useful information about the permeability or structure of the medium can be gleaned even from the q space data when it is not possible to apply large enough gradients to facilitate Fourier transforming to the more physically intuitive propagator space. For instance, the attenuation of the low q data yields the effective dispersion coefficient and the presence of a diffraction minimum in the data can indicate a structural dimension.

Fig. 3 shows both the q space data and the propagators for propane gas diffusing in the same bead pack used previously for water, i.e., 300 μm polystyrene beads. In q space a diffraction minimum is recognizable at a value corresponding to the inverse of the distance between the pores. This is a well known q space feature [1]. Fig. 3b illustrates clearly where the diffusive-diffraction minimum comes from (i.e., the dip at a distance equal to the pore size) and shows how the pores influence the propagator as diffusing molecules experience the pore walls. At a distance equivalent to the average pore separation we see the bleed-through effect as molecules break out into the next pore. We can also see indications of the third nearest pores.

For fluid diffusing with a self diffusion coefficient D_0 and contained within closed pores of dimension a, the result of the PGSTE experiment at a time $\Delta \gg a^2/D_0$ will be $E(q,\Delta) = |S_0(q)|^2$, where $S_0(q)$ is the Fourier power spectrum of the density $\rho(r)$ of the pore space. If the medium consists of interconnected pores then this theory must be extended to include the possibility of movement into adjacent pores. The pore-hopping theory of Callaghan et al. [24] addresses this situation. To approximate diffusion around spherical beads they assume an orientationally disordered pore glass with a variation in pore spacing of standard deviation ξ. The observation time Δ is assumed to allow full sampling of the initial pore and a probability of a jump into a nearest neighbor pore at a rate that depends on the interpore spacing b and the long range diffusion coefficient D_{eff} i.e., $\Delta \gg a^2/D_0$ and $\Delta \approx b^2/D_{\text{eff}}$. In this case the echo attenuation expands to a product of the local pore factor $S_0(q)$ and a factor $F(q,\Delta)$ which is sensitive to the temporal and spatial scales of the inter-pore hopping, i.e., $E(q,\Delta) = |S_0(q)|^2 F(q,\Delta)$. For the relevant case of a porous glass with pore spacing b and long time effective diffusion D_{eff} they derive

$$F(q,\Delta) = \exp\left[-\frac{6D_{\text{eff}}\Delta}{b^2+3\xi^2} \times\left(1-\exp(-2\pi^2q^2\xi^2)\frac{\sin(2\pi qb)}{2\pi qb}\right)\right], \qquad (2)$$

where ξ is the standard deviation in b.

This theory can be used to fit our q space diffraction curves. The solid lines in Fig. 3a show these fits and Table 1 lists the values used for the solid line fits. The fitted curves are $E(q,\Delta) = |S_0(q)|^2F(q,\Delta)$, where $|S_0(q)|$ is the Fourier power spectrum of the density of a spherical pore with diameter a. This model assumes spherical pores with diameter a that are much smaller than the pore separation b, in which case these spherical pores would be completely sampled by the diffusing species before the hop to the next pore took place. This model is obviously not exactly the case of diffusion between spherical beads, but it is a good approximation and was used in the original diffusive-diffraction paper for water in a similarly structured bead pack [24].

Our propane gas data compare well to the original diffusive-diffraction data for water in a similarly structured bead pack [24]. If we scale our curves for the larger beads and the faster diffusing gas, i.e., equal *Pe* number, they demonstrate the same structure and variations with Δ as those shown in the original paper [24] where water was diffusing among 10–30 μm beads. The variations in the fitted parameter values for the different observation times Δ are acceptable and comparable to those reported previously for a spherical bead pack [24].

Seymour and Callaghan [25] demonstrated that structure dimensions could be determined by sampling the porous medium convectively. This allows the use of shorter observation times or larger structures to be sampled in the available observation time by the flowing molecules. They observed diffraction peaks that corresponded to the pore size. In Fig. 4a we show q space diffraction peaks from gas flowing at 4 cm s^{-1} in 300 μm polystyrene beads at three observation times, $\Delta = 6$, 20, and 40 ms. These diffraction peaks have previously been observed for water flowing in smaller (10–100 μm) beads [20]. In Fig. 4b, these data are Fourier transformed to give the propagator representation. The propagators for the gas flowing at 4 cm s^{-1} in 300 μm polystyrene beads demonstrate the transition from the non-Gaussian situation at small observation times to a Gaussian at an observation time $\Delta = 150$ ms. The broad peak at zero could be due to molecules trapped in stagnant regions on the order of a pore size or could be thought of as the molecules that have not made the first jump to the next pore.

Table 1
Parameter values for the pore-hopping model of Callaghan et al. [24]

Observe time	70 ms	20 ms
D_{eff} ($m^2\,s^{-1}$)	2.20E − 06	2.20E − 06
Pore spacing, b	530 μm	400 μm
SD, ξ	100 μm	50 μm
Pore size, a	100 μm	100 μm

The fit predicts the correct values for the self-diffusion coefficient of the gas, D_{eff}, and the pore spacing b, i.e., approximately equal to the bead diameter. The model assumes the pore structure to be spheres connected by long and narrow throats, rather than short spaces between irregular pores, and this is reflected in an unrealistic estimation of pore size a. Our data show the same spatial and temporal variations as the liquid NMR data [24], albeit on different scales.

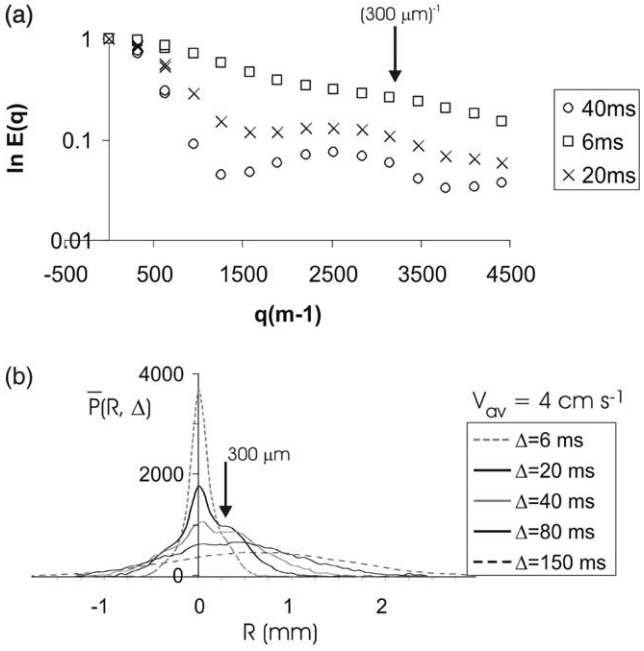

Fig. 4. (a) Diffraction peaks in the q space data from gas flowing at 4 cm s^{-1} in 300 μm polystyrene beads at three observation times, $\Delta = 6$, 20, and 40 ms. These diffraction peaks have previously been observed for water flowing in smaller (10–100 μm) beads [20]. (b) The data in Fig. 4a are Fourier transformed to give the propagator representation. The propagators for the gas flowing at 4 cm s^{-1} in 300 μm polystyrene beads demonstrate the transition from the non-Gaussian situation at small observation times to a Gaussian at $\Delta = 150$ ms. The broad peak at zero could be due to molecules trapped in stagnant regions on the order of a pore size or could be thought of as the molecules that have not made the first jump to the next pore.

In Fig. 5a, propagators are shown for the gas flowing at a faster rate of 50 cm s^{-1} through 300 μm polystyrene beads. As in Fig. 4b, they demonstrate the transition from the non-Gaussian situation at an observation time $\Delta = 3$ ms to a Gaussian at $\Delta = 20$ ms. In Fig. 5b, we show the gas flowing at several flow rates in the 300 μm polystyrene beads over the same observation time $\Delta = 6$ ms, showing the transition to Gaussian propagators for faster flow. The transition to Gaussian propagators at both long observation times Δ and faster flows is not the result of the same process. For long observation times all particles have time to diffuse out of their original pore and therefore experience the same average velocity for this time period. The transition to a Gaussian propagator at high velocities indicates the lack

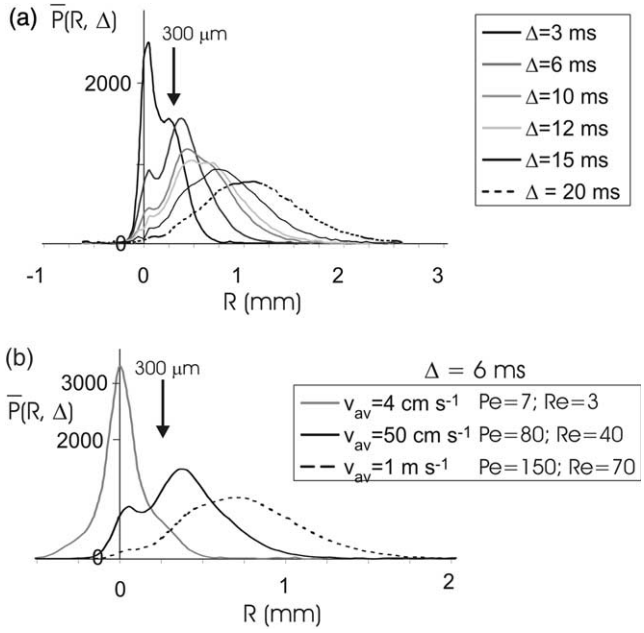

Fig. 5. (a) Propagators are shown for the gas flowing at a faster flow rate of 50 cm s^{-1} in 300 μm polystyrene bead pack. As in Fig. 4b, they demonstrate the transition from the non-Gaussian situation at an observation time $\Delta = 3$ ms to Gaussian at $\Delta = 20$ ms. (b) These propagators show the gas flowing at several flow rates in 300 μm polystyrene beads over the same observation time $\Delta = 6$ ms, showing the transition to a Gaussian propagator for fast enough times.

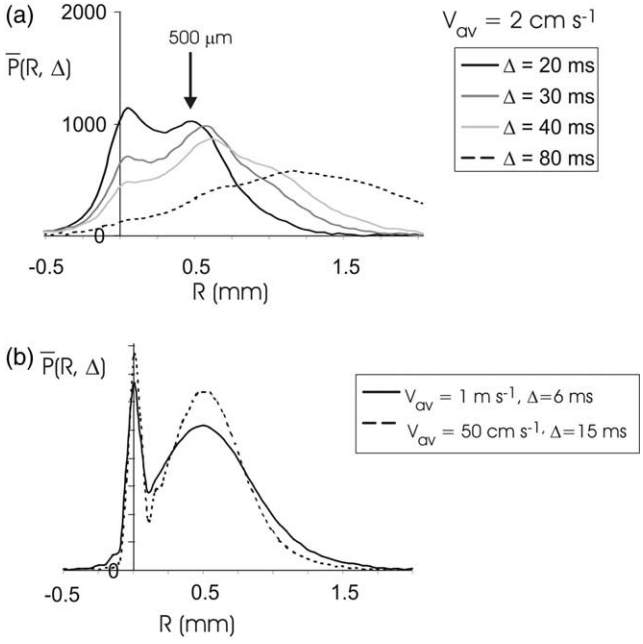

Fig. 6. (a) Propagators are shown for the gas flowing through 500 μm glass beads. These propagators show features similar to those observed in the 300 μm polystyrene bead pack. This indicates that the features observed are due to the pore structure and not due to wall or particle adsorption. (b) These propagators are for gas flowing through a pack of polydisperse and porous PVC particles with an average diameter of 100 μm. A large stagnant peak is still present at an observation time of $\Delta = 15$ ms and does not seem to depend on the flow rate. This indicates that there is a significant amount of gas trapped inside the porous PVC particles and these molecules must follow a tortuous pathway to reach the inter-particle pores and the flowing gas. Similarly structured propagators have been observed for water flowing through porous chromatography beads [13,15].

of truly stagnant regions (or dead end pores), and may be the result of some kind of microscopic Bernoulli effect.

In order to examine the possibility of any features of the data in the polystyrene being due to wall or bead adsorption of the gas, we show propagators obtained in a 500 μm glass bead pack for comparison in Fig. 6a. Similar features are observed for glass and polystyrene beads, albeit at a larger distance due to their larger diameter. This indicates that the features observed are due to the pore structure and not due to wall or particle adsorption.

The propagators in Fig. 6b are for gas flowing through a pack of polydispersed and porous PVC particles with an average diameter of 100 μm. A large stagnant peak is still present at an observation times $\Delta = 15$ ms and does not seem to depend on the flow rate. This indicates that there is a significant amount of gas that is trapped inside the porous PVC particles and these molecules must follow a tortuous pathway to reach the inter-particle pores and the flowing gas. Detailed analysis of hold-up dispersion in chromatography beads has been presented by Kandhai et al. [15]. The propagators they observe are similar to propagators we obtained for propane gas flowing through a column of PVC particles. The PVC particles are porous and a large stagnant peak in the propagator demonstrates that a significant amount of the gas remains separated from the flowing gas inside these particles. They diffuse out of the particles and exchange with the flowing gas in approximately 600 ms, indicating a fairly tortuous pathway.

A narrow (stagnant) peak and a broader (flowing) peak in the propagator space can make themselves apparent, even in q space, by different slopes at large and small q values, respectively. When these large and small q value data can be resolved, it is possible to determine the scaling of these dispersion mechanisms with Peclet numbers and observation times and compare them to those established in the literature.

6. Conclusion

NMR studies of gas phase flow and diffusion in porous materials enable structures to be investigated on a completely different distance scale than that accessible with NMR of liquid phase fluids. Different combinations of Reynolds and Peclet numbers are accessible in the NMR observation time window for these two experiments. Thermally polarized gas NMR is limited by low signal to noise ratios because gas densities are on the

order of 1000 times smaller than liquid densities. However we use molecules with multiple NMR active nuclei that have short T_1's and operate at elevated pressures to overcome some of the losses. Thermally polarized gases have advantages over hyperpolarized gases in the ease of preparation, well-defined polarization, and the immunity from surface relaxation. Propane in polystyrene has a T_1 of 500 ms, although the T_2 is reduced to a few ms due to susceptibility effects. We used stimulated echo sequences to successfully obtain propagators of gas in a bead pack out to observation times of 300 ms. There is also the possibility to adjust the diffusivity and hence Peclet number of the gas by doing pressure dependent studies.

Acknowledgments

The authors wish to thank Eiichi Fukushima for input and guidance with the manuscript and acknowledge the support of the US Department of Energy, Office of Basic Energy Sciences, Division of Materials Sciences and Engineering, via Grant No. DE-FG03-93ER14316. This sponsorship does not constitute endorsement by the US Department of Energy of the views expressed in this article.

References

[1] P.T. Callaghan, Principles of Nuclear Magnetic Resonance Microscopy, Oxford University Press, New York, 1991.
[2] R.W. Mair, D.G. Cory, S. Peled, C.-H. Tseng, S. Patz, R.L. Walsworth, Pulsed-field-gradient measurements of time dependent gas diffusion, J. Magn. Reson. 135 (1998) 478–486.
[3] R.W. Mair, C.-H. Tseng, G.P. Wong, D.G. Cory, R.L. Walsworth, Magnetic resonance imaging of convection in laser-polarized xenon, Phys. Rev. E 61 (2000) 2741–2748.
[4] L.G. Kaiser, J.W. Logan, T. Meersman, A. Pines, Dynamic NMR microscopy of gas phase Poiseuille flow, J. Magn. Reson. 149 (2001) 144–148.
[5] I.V. Koptyug, A.V. Matveev, S.A. Altobelli, NMR studies of hydrocarbon gas flow and dispersion, Appl. Magn. Reson. 22 (2002) 187–200.
[6] M. Bencsik, C. Ramanathan, Method for measuring local hydraulic permeability using magnetic resonance imaging, Phys. Rev. E 63 (2001), 065302(R)-4.
[7] D.O. Kuethe, A. Caprihan, E. Fukushima, R.A. Waggoner, Imaging lungs using fluorinated gases, Magn. Reson. Med. 39 (1998) 85–88.
[8] I.V. Koptyug, S.A. Altobelli, E. Fukushima, A.V. Matveev, R.Z. Sagdeev, Thermally polarised 1H NMR microimaging studies of liquid and gas flow in monolithic catalysts, J. Magn. Reson. 147 (2000) 36–42.
[9] S.D. Beyea, A. Caprihan, C.F.M. Clewett, S.J. Glass, Spatially resolved adsorption isotherms of thermally polarized perfluorinated gases in Y-TZP ceramic materials with NMR imaging, Appl. Magn. Reson. 22 (2002) 175–186.
[10] P.T. Callaghan, S.L. Codd, J.D. Seymour, Spatial coherence phenomena arising from translational spin motion in gradient spin echo experiments, Concepts Magn. Reson. 11 (1999) 181–202.
[11] S. Stapf, S.-I. Han, C. Heine, B. Bluemich, Spatiotemporal correlations in transport processes determined by multiple pulsed field gradient experiments, Concepts Magn. Reson. 14 (2002) 172–211.
[12] M.D. Hurlimann, L. Venkataramanan, C. Flaum, NMR in grossly inhomogeneous fields: new quantitative measurement of diffusion–relaxation distribution function, ENC Conference Asilomar, 2002.
[13] U. Tallarek, F.J. Vergeldt, H. Van As, Stagnant mobile phase mass transfer in chromatographic media: intraparticle diffusion and exchange kinetics, J. Phys. Chem. B 103 (1999) 7654–7664.
[14] J.J. Tessier, K.J. Packer, The characterization of multiphase fluid transport in a porous solid by pulsed gadient stimulated echo nuclear magnetic resonance, Phys. Fluids 10 (1998) 75–85.
[15] D. Kandhai, D. Hlushkou, A.G. Hoekstra, P.M.A. Sloot, H. Van As, U. Tallarek, Influence of stagnant zones on transient and asymptotic dispersion in macroscopically homogeneous porous media, Phys. Rev. Lett. 88 (2002) 234501–234504.
[16] B. Bluemich, P.T. Callaghan, R.A. Damion, S.-I. Han, A.A. Khrapitchev, K.J. Packer, S. Stapf, Two-dimensional NMR of velocity exchange: VEXSY and SERPENT, J. Magn. Reson. 151 (2001) 162–167.
[17] J. Salles, J.-F. Thovert, L. Delannay, J.-L. Auriault, P.M. Adler, Taylor dispersion in porous media, Phys. Fluids 5 (1993) 2348–2376.
[18] G.I. Taylor, Diffusion by continuous movements, Proc. Lond. Math. Soc. 20 (1921) 196–212.
[19] M.H.G. Amin, S.J. Gibbs, R.J. Chorley, K.S. Richards, T.A. Carpenter, L.D. Hall, Study of flow and hydrodynamic dispersion in a porous medium using pulsed-field-gradient magnetic resonance, Proc. Roy. Soc. Lond. A 453 (1997) 489–513.
[20] J.D. Seymour, P.T. Callaghan, Generalized approach to NMR analysis of flow and dispersion in porous medium, AIChE J. 43 (1997) 2096–2111.
[21] B. Manz, L.F. Gladden, P.B. Warren, Flow and dispersion in porous media: Lattice–Boltzmann and NMR studies, AIChE J. 45 (1999) 1845–1854.
[22] S. Stapf, K.J. Packer, R.G. Graham, J.-F. Thovert, P.M. Adler, Spatial correlations and dispersion for fluid transport through packed glass beads studied by pulsed field-gradient NMR, Phys. Rev. E 58 (1998) 6206–6221.
[23] L. Lebon, L. Oger, J. Leblond, J.P. Hulin, J.P. Martys, N.S. Schwartz, Pulsed gradient NMR measurements and numerical simulation of flow velocity distribution in sphere packings, Phys. Fluids 8 (1996) 293–301.
[24] P.T. Callaghan, A. Coy, T.P.J. Halpin, D. MacGowan, K.J. Packer, F.O. Zelaya, Diffusion in porous systems and the influence of pore morphology in pulsed gradient spin echo nuclear magnetic resonance studies, J. Chem. Phys. 97 (1992) 651–662.
[25] J.D. Seymour, P.T. Callaghan, Flow-diffraction structural characterization and measurement of hydrodynamic dispersion in porous media by PGSE NMR, J. Magn. Reson. A 122 (1996) 90–93.